J|A|C|S
ARTICLES
Published on Web 02/13/2004

Investigation of Noncovalent Interactions in Deprotonated Peptides: Structural and Energetic Competition between Aggregation and Hydration

Dengfeng Liu, Thomas Wyttenbach, Catherine J. Carpenter, and Michael T. Bowers*

Contribution from the Department of Chemistry and Biochemistry, University of California at Santa Barbara, California 93106

Received October 31, 2003; E-mail: bowers@chem.ucsb.edu

Abstract: Noncovalent peptide−peptide and peptide−water interactions in small model systems were examined using an electrospray mass spectrometer equipped with a high-pressure drift cell. The results of these aggregation and hydration experiments were interpreted with the aid of molecular mechanics (MM) and density functional theory (DFT) calculations. The systems investigated include bare deprotonated monomers and dimers $[P_{1,2}-H]^-$ and hydrated deprotonated monomers and dimers $[P_{1,2}-H]^-\cdot(H_2O)_n$ for the peptides dialanine (P = AA) and diglycine (P = GG). Mass spectra indicated that both peptides AA and GG form exclusively dimer ions in the electrospray process. Monomeric ions were generated by high-energy injection of the dimers into the drift cell. Temperature-dependent hydration equilibrium experiments carried out in the drift cell yielded water binding energies ranging from 11.7 (first water molecule) to 7.1 kcal/mol (fourth water) for $[AA-H]^-$ and 11.0 to 7.4 kcal/mol for $[GG-H]^-$. The first water molecule adding to the dimer ions $[AA-H]^-\cdot(AA)$ and $[GG-H]^-\cdot(GG)$ is bound by 8.4 and 7.5 kcal/mol, respectively. The hydration mass spectra for the monomers and dimers provide a means to compare the ability of water and a neutral peptide to solvate a deprotonated peptide $[P-H]^-$. The data indicate that a similar degree of solvation is achieved by four water molecules, $[P-H]^-\cdot(H_2O)_4$, or one neutral peptide, $[P-H]^-\cdot(P)$. Temperature-dependent kinetics experiments yielded activation energies for dissociation of the dimers $[AA-H]^-\cdot(AA)$ and $[GG-H]^-\cdot(GG)$ of 34.9 and 32.2 kcal/mol, respectively. MM and DFT calculations carried out for the dialanine system indicated that the dimer binding energy is 24.3 kcal/mol, when the $[AA-H]^-$ and AA products are relaxed to their global minimum structures. However, a value of 38.9 kcal/mol is obtained if $[AA-H]^-$ and AA dissociate but retain the structures of the moieties in the dimer, suggesting the transition state occurs early in the dissociation process. Similar results were found for the diglycine dimer.

Introduction

Noncovalent interactions play a dominant role in protein conformation and the folding process. Because of the important relationship between function and shape in biomolecules, noncovalent interactions are crucial to the biological activity of many proteins. The ionic hydrogen bond is one of the most important noncovalent interactions found in biosystems and, as such, has attracted significant attention recently from chemists and biochemists. In an ionic hydrogen bond, a charged group in a biomolecule is solvated by a hydrophilic group from the biomolecule itself or by another molecule.

A number of polar groups found in biomolecules, such as the hydroxyl group, make excellent charge solvents by forming intramolecular hydrogen bonds. An important feature of this self-solvation is that all the functional groups are within the same molecule so that the formation of the hydrogen bonds causes the biomolecules to fold and become more compact. In nature, most biomolecules are found in an aqueous environment. Water molecules also make good charge solvation groups because of their ability to be both hydrogen bond donors and acceptors. Many studies have illustrated water's unique role in the conformation of biomolecules,[1,2] in charge stabilization,[3−5] and even as the key to bioactivity in some cases.[6] In contrast to self-solvation, hydration can disrupt intramolecular interactions, thereby making biomolecules relatively less compact.

Undoubtedly water molecules will compete with intramolecular hydrophilic groups to solvate charged groups and affect biomolecule conformation. This competition plays an important role in protein folding. In the folding process, hydrogen bonds between the unfolded protein and water are broken and new intramolecular interactions are formed. Experimental and theoretical results show that water molecules are "squeezed out" in the protein folding process.[7] The protein

(1) Madhumalar, A.; Bansal, M. *Biophys. J.* **2003**, *85*, 1805.
(2) Wu, C.-C.; Chaudhuri, C.; Jiang, J. C.; Lee, Y. T.; Chang, H.-C. *Mol. Phys.* **2003**, *101*, 1285.
(3) Jensen, J. H.; Gordon, M. S. *J. Am. Chem. Soc.* **1995**, *117*, 8159.
(4) Jensen, J. H.; Gordon, M. S. *Acc. Chem. Res.* **1996**, *29*, 536.
(5) Wyttenbach, T.; Paizs, B.; Barran, P.; Breci, L.; Liu, D.; Suhai, S.; Wysocki, V. H.; Bowers, M. T. *J. Am. Chem. Soc.* **2003**, *125*, 13768.
(6) Pocker, Y. *Cell. Mol. Life Sci.* **2000**, *57*, 1008.
(7) Jacob, M. H.; Saudan, C.; Holtermann, G.; Martin, A.; Perl, D.; Merbach, A. E.; Schmid, F. X. *J. Mol. Biol.* **2002**, *318*, 837.

bioactivity depends on the balance between self-solvation and hydration. Hence an understanding of this competition is very important for future protein folding research.

Development of soft ionization methods, in particular matrix-assisted laser desorption ionization (MALDI)[8,9] and electrospray ionization (ESI)[10] have led to a revolution in the application of mass spectrometry to macromolecular systems. Many biomolecules, such as peptides, proteins, and nucleic acids, which were inaccessible before, are now common mass spectrometry research subjects. An important feature of the soft ionization methods is that they allow, under certain conditions, the transfer of noncovalently bound complexes into the gas phase.[11−15] As a result, many mass spectrometry techniques are being used to investigate noncovalent bonds in biochemical systems. The advantage of investigating biomolecules in the gas phase is that it allows one to observe bare biomolecules separated from the bulk solvent. In this way, noncovalent interactions between and within biomolecules can be distinguished from the numerous solvent effects. In addition, controlled numbers of solvent molecules can be added to biomolecule complexes. As a result, hydration interactions can also be studied essentially one water molecule at a time in the gas phase. Thermodynamic properties of hydration can be measured as function of the number of adsorbed water molecules, and the effects of the adsorbed water on the conformation of the biomolecule can be examined.

Two types of intermolecular noncovalent interactions, which are frequently competing with each other, are of particular interest in biochemistry: the interaction between two biomolecules (docking, aggregation) and the interaction between water and a biomolecule (hydration). Gas-phase experiments designed to investigate the energetics of biomolecule−biomolecule interactions generally focus on the dissociation reactions of noncovalently bound complexes. One example of this kind of experiment is blackbody infrared radiative dissociation (BIRD),[16−18] in which unimolecular dissociations are probed using FT-ICR mass spectrometry. Activation energies can be determined from measurements of dissociation rates as a function of the temperature. BIRD experiments have been successful in investigating many biomolecule dissociation reactions with activation energies in the range of 10−40 kcal/mol.

Gas-phase experiments dealing with hydration can be divided into two groups: those allowing water to remain on the biomolecule ion when it is produced by ESI and those where water is added to a dehydrated biomolecule. Several groups have pursued the first approach using ESI to produce microsolvated protein ions.[19−23] Results show that some peptides, such as doubly protonated gramicidin S, favor solvation by specific numbers of water molecules.[20−22] It has been suggested that these favored species correspond to stable solvation shells around the charge sites. However, other ions, such as doubly protonated bradykinin, do not display any preference.[22] Energetic and structural information of hydrated species can be obtained from BIRD experiments as described above.[23]

In the second approach for studying hydration, biomolecule ions are formed dehydrated, in the gas phase, and are rehydrated by exposing them to water vapor. The number of adsorbed water molecules can be determined by mass spectrometry, and if equilibrium is established, equilibrium constants can be determined. An equilibrium constant measured at a single temperature provides $\Delta G°$ for hydration at that temperature. An equilibrium constant measured as a function of temperature provides $\Delta H°$ and $\Delta S°$. This approach was used in a number of studies[24−28] including our previous work[29] in which a series of peptides were investigated. We found that under the same experimental conditions, the number of water molecules which bind to a peptide is primarily dependent on the peptide's charge state. This result has led us to the systematic investigation of the interaction between water and the three types of charge-carrying groups found in peptides: the protonated amino and guanidino groups and the anionic carboxylate group. Initial results for the two protonated groups are already published[29] and a second study comparing hydration of free amines with amines engaged in intramolecular hydrogen bonds is forthcoming.[30]

In this paper we will focus on the carboxylate group. We will present results for two deprotonated dipeptides: dialanine $[AA-H]^-$ and diglycine $[GG-H]^-$. The study consists of three parts. First, peptide aggregation is addressed by investigating the interactions of the two monomer subunits in the peptide dimers $[AA-H]^-\cdot(AA)$ and $[GG-H]^-\cdot(GG)$. Using drift tube mass spectrometry methods, kinetics experiments were performed to measure dissociation activation energies for these dimers (reaction 1, where the peptide P = AA or GG).

$$[P-H]^-\cdot(P) \rightarrow [P-H]^- + P \quad (1)$$

Second, peptide hydration is addressed by investigating the interactions of the deprotonated dipeptide monomers and dimers with water. Equilibrium experiments were performed to measure binding energies of water with both the monomers and dimers (reaction 2).

$$[P_{1,2}-H]^-\cdot(H_2O)_{n-1} + H_2O \leftrightharpoons [P_{1,2}-H]^-\cdot(H_2O)_n \quad (2)$$

Third, density functional theory (DFT) calculations for selected species involved in reactions 1 and 2 were performed to gain further insight into the experimental results. These experimental and theoretical results allow us to compare self-solvation and hydration and study the competition between them.

(8) Karas, M.; Hillenkamp, F. *Anal. Chem.* **1988**, *60*, 2288.
(9) Hillenkamp, F. *Adv. Mass Spectrom.* **1989**, *11A*, 354.
(10) Fenn, J. B.; Mann M.; Meng, C. K.; Wong, S. F. *Science* **1989**, *246*, 64.
(11) Ganem, B.; Li, T.; Henion, J. D. *J. Am. Chem. Soc.* **1991**, *113*, 6294.
(12) Ganem, B.; Li, T.; Henion, J. D. *J. Am. Chem. Soc.* **1991**, *113*, 7818.
(13) Winston, R. L.; Fitzgerald, M. C. *Mass Spectrom. Rev.* **1997**, *16*, 165.
(14) Loo, J. A. *Mass Spectrom. Rev.* **1997**, *16*, 1.
(15) Schalley, C. A. *Mass Spectrom. Rev.* **2001**, *20*, 253.
(16) Price, W. D.; Schnier, P. D.; Williams, E. R. *Anal. Chem.* **1996**, *68*, 859.
(17) Schnier, P. D.; Price, W. D.; Jockusch, R. A.; Williams, E. R. *J. Am. Chem. Soc.* **1996**, *118*, 7178.
(18) Price, W. D.; Schnier, P. D.; Jochusch, R. A.; Strittmatter, E. F.; Williams, E. R. *J. Am. Chem. Soc.* **1996**, *118*, 10640.
(19) Chowdhury, S. K.; Katta, V.; Chait, B. T. *Rapid Commun. Mass Spectrom.* **1990**, *4*, 81.
(20) Rodriguez-Cruz, S. E.; Klassen, J. S.; Williams, E. R. *J. Am. Soc. Mass Spectrom.* **1997**, *8*, 565.
(21) Rodriguez-Cruz, S. E.; Klassen, J. S.; Williams, E. R. *J. Am. Soc. Mass Spectrom.* **1999**, *10*, 958.
(22) Lee, S.-W.; Freivogel, P.; Schindler, T.; Beauchamp, J. L. *J. Am. Chem. Soc.* **1998**, *120*, 11758.
(23) Jockusch, R. A.; Lemoff, A. S.; Williams, E. R. *J. Phys. Chem. A* **2001**, *105*, 10929.
(24) Meot-Ner, M.; Field, F. H. *J. Am. Chem. Soc.* **1974**, *96*, 3168.
(25) Klassen, J. S.; Blades, A. T.; Kebarle, P. *J. Phys. Chem.* **1995**, *99*, 15509.
(26) Woenckhaus, J.; Mao, Y.; Jarrold, M. F. *J. Phys. Chem. B* **1997**, *101*, 847.
(27) Woenckhaus, J.; Hudgins, R. R.; Jarrold, M. F. *J. Am. Chem. Soc.* **1997**, *119*, 9586.
(28) Kohtani, M.; Jarrold, M. F. *J. Am. Chem. Soc.* **2002**, *124*, 11148.
(29) Liu, D.; Wyttenbach, T.; Barran, P. E.; Bowers, M. T. *J. Am. Chem. Soc.* **2003**, *125*, 8458.
(30) Liu, D.; Wyttenbach, T.; Bowers, M. T. Manuscript in preparation.

Methods

An ESI mass spectrometer that incorporates a drift cell was used to perform both kinetics and equilibrium experiments. The key difference between the two experiments performed for this study is the type of reaction that takes place in the drift cell. Each method will be addressed separately after a brief description of the instrumentation. A detailed description of the instrument can be found in the literature.[31]

Instrumentation. Ions are produced by nano-electrospray ionization (ESI) and transported into a high-vacuum chamber through a metal capillary. A metalized glass needle is used as a spray tip and is operated without any back-pressure. The voltage on the spray needle is typically −700 to −1000 V with respect to the capillary for negative ions and +1000 to +1300 V for positive ions. An ion funnel acts as the interface between the ESI source and the ion drift cell located in a high-vacuum chamber. The funnel is a high-transmission radio frequency (rf) ion guide that has three functions. First, it compresses the divergent stream of ions exiting the capillary down to a small diameter. Second, it moves the ions from the source region to the drift cell without the use of high-acceleration fields, thus avoiding high-energy ion−neutral collisions. Third, for experiments requiring ion pulses, the funnel can be used to convert the continuous ion beam from the ESI source into a pulsed beam. This is accomplished by raising the potential of the last lens of the funnel, thus trapping the ions in the funnel, and periodically pulsing it down for short periods of time (10 μs) to let pulses of ions exit.

After leaving the funnel, the ions are injected into a drift cell filled with ~5 Torr of helium or 0.2−2 Torr of water vapor, depending on the type of experiment to be performed. Ions travel through the cell under the influence of a weak electric field (10−25 V cm^{-1}). Depending on the experimental conditions, ions either drift in helium without reacting (yielding cross sections), dissociate in helium (reaction 1), or cluster with water molecules (reaction 2) in the drift cell. The cell temperature can be increased above room temperature by electrical heaters or cooled by the flow of liquid-nitrogen-cooled nitrogen gas and is measured by a Pt-resistor and three thermocouples in various places in and around the copper cell. Product ions are analyzed in the quadrupole mass filter following the drift cell and detected by a channel electron multiplier.

The energy with which the ions are injected into the drift cell can also be changed by varying the voltage difference between the cell and the ion funnel. Usually low energies are used. However, at high injection energies isomerization and dissociation can be induced by high-energy collisions. This will be useful when studying hydration of $[P-H]^-$ ions.

All the samples were purchased from Sigma (St. Louis, MO) and used without further purification. Samples were typically sprayed from a ~100 μM solution (water:acetonitrile:ammonium hydroxide, 49:49:2 for negative ions; or water:acetonitrile:trifluoroacetic acid, 50:50:0.1 for positive ions).

Kinetics Experiments. The reaction time for dissociation is determined by the dimer ion mobility K and the voltage V across the drift cell.[32] Using eq 3, which relates the drift velocity v_d to the electric field E, we arrive at eq 4, where L is the drift length and K_0 is the "reduced" mobility defined in eq 5 with values of 760 Torr for P_0 and 273.15 K for T_0.

$$v_d = KE \tag{3}$$

$$t_d = \frac{L}{v_d} = \frac{L}{KE} = \frac{L^2 T_0}{K_0 P_0 T}\frac{P}{V} \tag{4}$$

$$K_0 = K\frac{P}{P_0}\frac{T_0}{T} \tag{5}$$

The quantity measured in the experiment (using an ion pulse) is the arrival time of the ions at the detector t_a, which is equal to $t_d + t_0$, where t_0 is the amount of time the ions spend outside the drift cell. Plotting t_a vs P/V for a given temperature yields a straight line with an intercept equal to t_0 and a slope that is inversely proportional to the reduced mobility K_0. The reaction time, i.e., the drift time t_d, can be obtained by subtracting t_0 from the arrival time t_a. Typical drift times are approximately 300 μs, but t_d can be adjusted from 150 to 1500 μs, depending on the drift voltage used.

Rate constants for reaction 1 can be obtained by measuring the intensity of the dimer ions as a function of time using eq 6 (first-order kinetics).

$$\ln\left(\frac{[\text{dimer}]_0}{[\text{dimer}]_t}\right) = kt \tag{6}$$

The ratio of dimer ion concentration at time 0 to that at time t can be derived from the intensity ratio of the sum of dimer and monomer to the dimer ion at time t (eq 7), where α accounts for mass discrimination effects (ideally $\alpha = 1$).

$$\frac{[\text{dimer}]_0}{[\text{dimer}]_t} = \frac{I_{\text{dimer}} + \alpha I_{\text{monomer}}}{I_{\text{dimer}}} \tag{7}$$

Plotting $\ln[(I_{\text{dimer}} + \alpha I_{\text{monomer}})/I_{\text{dimer}}]$ vs reaction time t gives a straight line with a slope equal to the rate constant k. The data presented in this work yield straight lines for $\alpha = 1$, indicating that mass discrimination is minimal. An Arrhenius plot of $\ln k$ versus $1/T$ (eq 8) yields the activation energy E_a (slope) and the preexponential factor A (intercept) for reaction 1.

$$\ln k = \ln A - \frac{E_a}{RT} \tag{8}$$

Arrhenius plots obtained in this work yield straight lines indicating that the dissociation processes occur in the rapid exchange (REX) limit.[33] This is expected as the collision frequency at 5 Torr of helium is approximately 2×10^8 s^{-1}, which exceeds the dissociation rate constants obtained in this work by several orders of magnitude. This ensures that the high-energy states of dimers lost due to dissociation are efficiently repopulated and that the dimers maintain a Boltzmann distribution throughout the drift cell.

For completeness we would like to note that in the past we have used a different method to obtain the rate constants for reactions occurring in the drift cell.[31,34−36] In that method, a pulse of ions is injected into the helium-filled drift cell. Because the dimer and monomer have different mobilities, they drift through the cell at different velocities, with the monomer arriving at the detector first. The quadrupole following the drift cell is tuned to the monomer product ion, and an arrival time distribution (ATD) is measured. The ATD is a plot of ion intensity vs arrival time at the detector. The shape of this distribution depends on the rate at which the dimer dissociates to monomer. By matching the ATD with a theoretical model, the rate constant can be determined. This is the method of choice when both reactant and product have identical mass-to-charge ratios. Here, however, the direct measurements of dimer and monomer abundances give more reliable results with smaller error bars. Hence, although both methods give results that are in general agreement with each other, we report only results obtained by the first method.

(31) Wyttenbach, T.; Kemper, P. R.; Bowers, M. T. *Int. J. Mass. Spectrom.* **2001**, *212*, 13.
(32) Mason, E. A.; McDaniel, E. W. *Transport Properties of Ions in Gases*; Wiley: New York, 1988.
(33) Price, W. D.; Schnier, P. D.; Jockusch, R. A.; Strittmatter, E. F.; Williams, E. R. *J. Am. Chem. Soc.* **1996**, *118*, 10640.
(34) Gidden, J.; Bowers, M. T. *J. Am. Soc. Mass Spectrom.* **2003**, *14*, 161.
(35) Gidden, J.; Bowers, M. T. *Eur. Phys. J. D* **2002**, *20*, 409.
(36) Gidden, J.; Wyttenbach, T.; Batka, J. J.; Weis, P.; Jackson, A. T.; Scrivens, J. H.; Bowers, M. T. *J. Am. Soc. Mass Spectrom.* **1999**, *10*, 883.

Equilibrium Experiments. In the equilibrium experiments, the mixture of hydrated ions $[P_{1,2}-H]^-\cdot(H_2O)_n$ leaving the drift cell is mass-analyzed. Mass spectra obtained at different drift times are identical, confirming that equilibrium is established inside the cell under the conditions used. Because the intensity I_n of the $[P_{1,2-}H]^-\cdot(H_2O)_n$ mass peak is proportional to the ion's concentration,[37] the ratio I_n/I_{n-1} yields the equilibrium constant K_n (eq 9).

$$K_n = \frac{I_n}{I_{n-1}} \frac{1}{P(H_2O)} \tag{9}$$

In eq 9, $P(H_2O)$ is the known water pressure. The water pressure is limited by the pumping capacity and, at low temperatures, by the water vapor pressure over ice. Maximum water pickup is achieved at ~260 K, a compromise between low temperature and still-reasonable water vapor pressure (~1.3 Torr). Measuring K_n as a function of temperature yields values for the enthalpy ΔH_n° and entropy ΔS_n° of hydration. Equation 10 is used to convert equilibrium constants to standard-state free energies ΔG_n° of hydration, and according to eq 11, a plot of ΔG_n° vs T yields a straight line with an intercept equal to ΔH_n° and a slope equal to $-\Delta S_n^\circ$. The ΔH_n° and ΔS_n° values determined by this method are valid over the temperature range of the experiment.

$$\Delta G_n^\circ = -RT \ln K_n \tag{10}$$

$$\Delta G_n^\circ = \Delta H_n^\circ - T\Delta S_n^\circ \tag{11}$$

Theoretical Methods. In an attempt to theoretically understand experimental trends, the dissociation and hydration processes have also been studied by computer simulations using molecular mechanics methods combined with density functional theory (DFT). For the molecular mechanics calculations, the AMBER 7 suite of programs was employed together with the standard AMBER force field to obtain the lowest-energy candidate structures. This was achieved using a simulated annealing protocol identical to that previously described.[38] Selected structures obtained by molecular mechanics were further optimized by DFT methods at the B3LYP/ 6-31G* level using the GAUSSAIN98 software package.[39] All binding energies reported here include the counterpoise correction[40] to account for basis set superposition errors (BSSE). Given the large size of the systems studied, which makes frequency calculations prohibitively difficult, no attempt was made to correct for zero-point vibrational energies.

Cross Sections. Orientation-averaged cross sections for theoretical structures are calculated by a sophisticated projection approximation method previously described.[41,42] Atomic radii used for the projection are adjusted as a function of molecule size[42] and temperature using a (12,6,4) ion−helium interaction potential.[41]

Experimental cross sections σ are deduced from the reduced mobility K_0 (eq 4) using the relationship in eq 12,[32] where e is the charge of the ion, N_0 the particle density at 760 Torr and 273.15 K, μ the reduced mass (ion−helium), k_B the Boltzmann constant, and T the temperature.

$$K_0 = \frac{3e}{16N_0}\left(\frac{2\pi}{\mu k_B T}\right)^{1/2}\frac{1}{\sigma} \tag{12}$$

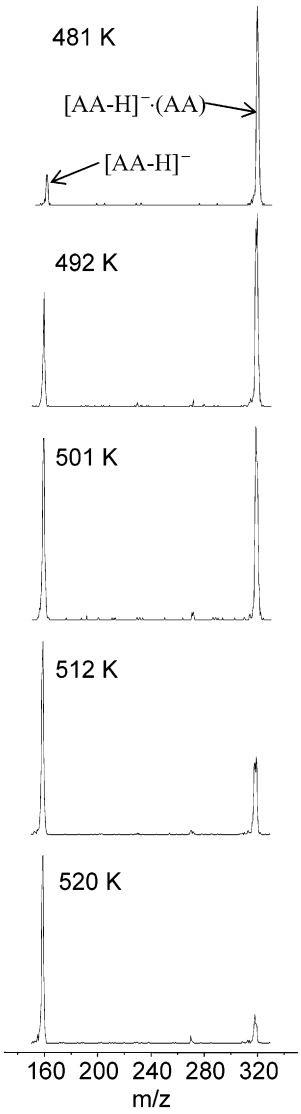

Figure 1. Mass spectra of deprotonated dialanine dimer dissociation, $[AA-H]^-\cdot(AA) \rightarrow [AA-H]^- + AA$, at different drift cell temperatures. At all temperatures, the cell pressure (5 Torr of helium) and drift voltage (60 V) were the same to ensure that the reaction time was the same for each measurement.

Results and Discussion

Noncovalent Bonds between Peptides. In our experiment, negative ion ESI of dialanine and diglycine solutions produced only deprotonated dipeptide dimers at room temperature. No deprotonated monomer formation was observed. However, dimer dissociation to monomer (reaction 1) in the reaction cell was found to occur at temperatures above 470 K for both dialanine and diglycine. Figure 1 shows the mass spectra obtained at different temperatures for deprotonated dialanine dimer dissociation. The dimer-to-monomer intensity ratio gradually decreases with increasing temperature from ~9 at 480 K to ~0.1 at 520 K.

The dimer-to-monomer intensity ratio also depends on reaction time. As described in Methods, reaction time is

(37) Mass discrimination effects, which were small in the kinetics experiment, are even smaller here because the masses of the two species $[P_{1,2}-H]^-\cdot(H_2O)_n$ and $[P_{1,2}-H]^-\cdot(H_2O)_{n+1}$ are very similar.
(38) Wyttenbach, T.; Helden, G. v.; Bowers, M.T. *J. Am. Chem. Soc.* **1996**, *118*, 8355
(39) Frisch, M. J.; Trucks, G. W.; Schlegel, H. B.; Scuseria, G. E.; Robb, M. A.; Cheeseman, J. R.; Zakrzewski, V. G.; Montgomery, J. A., Jr.; Stratmann, R. E.; Burant, J. C.; Dapprich, S.; Millam, J. M.; Daniels, A. D.; Kudin, K. N.; Strain, M. C.; Farkas, O.; Tomasi, J.; Barone, V.; Cossi, M.; Cammi, R.; Mennucci, B.; Pomelli, C.; Adamo, C.; Clifford, S.; Ochterski, J.; Petersson, G. A.; Ayala, P. Y.; Cui, Q.; Morokuma, K.; Malick, D. K.; Rabuck, A. D.; Raghavachari, K.; Foresman, J. B.; Cioslowski, J.; Ortiz, J. V.; Baboul, A. G.; Stefanov, B. B.; Liu, G.; Liashenko, A.; Piskorz, P.; Komaromi, I.; Gomperts, R.; Martin, R. L.; Fox, D. J.; Keith, T.; Al-Laham, M. A.; Peng, C. Y.; Nanayakkara, A.; Gonzalez, C.; Challacombe, M.; Gill, P. M. W.; Johnson, B. G.; Chen, W.; Wong, M. W.; Andres, J. L.; Head-Gordon, M.; Replogle, E. S.; Pople, J. A. *GAUSSIAN98*; Gaussian, Inc.: Pittsburgh, PA, 1998.
(40) Boys, S. F.; Bernardi, F. *Mol. Phys.* **1970**, *19*, 553.
(41) Wyttenbach, T.; von Helden, G.; Batka, J. J.; Carlat, D.; Bowers, M. T. *J. Am. Soc. Mass Spectrom.* **1997**, *8*, 275.
(42) Wyttenbach, T.; Witt, M.; Bowers, M. T. *J. Am. Chem. Soc.* **2000**, *122*, 3458.

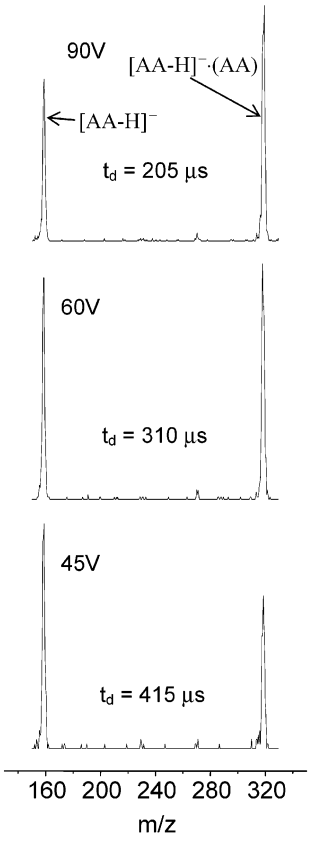

Figure 2. Mass spectra of deprotonated dialanine dimer dissociation, $[AA-H]^-\cdot(AA) \rightarrow [AA-H]^- + AA$, at different drift voltages. For all three measurements, the drift cell temperature was 501 K and the He pressure was 5 Torr.

controlled by adjusting the drift voltage. Figure 2 shows the mass spectra for dialanine dimer measured at three different drift voltages, all at 501 K. Rate constants for the dialanine and diglycine dimer dissociations were determined by measuring the dimer-to-monomer ratio as a function of time at a constant temperature. All kinetics data for dialanine dimer dissociation are summarized in Figure 3. The slopes of these lines give the dissociation rate constants at each temperature. Analogous experiments were carried out for $[GG-H]^-\cdot(GG)$, and Arrhenius plots for both systems are presented in Figure 4. From the slope of the line in Figure 4a, we obtain a dissociation activation energy (E_a) of 34.9 ± 1.4 kcal/mol for $[AA-H]^-\cdot(AA)$. We derive a similar value of 32.2 ± 2.1 kcal/mol for $[GG-H]^-\cdot(GG)$ dissociation from the plot in Figure 4b. The two dissociation reactions also have similar preexponential factors (A) obtained from the y-intercepts: $\log(A) = 18.5$ for dialanine and $\log(A) = 17.0$ for diglycine. All of these Arrhenius parameters are summarized in Table 1 with the error bars corresponding to the standard deviations of the linear regression fits to the experimental data.

There are no prior measurements of these Arrhenius parameters in the literature. However the dissociation of $[A+H]^+\cdot(A)$ to $[A+H]^+ + A$ has been studied using the BIRD technique.[43] We measured the activation energy for this positive ion reaction using the methods described here and obtained 21.9 ± 0.3 kcal/mol in good agreement with the BIRD value of 21.2

(43) Price, W. D.; Schnier, P. D.; Williams, E. R. *J. Phys. Chem. B* **1997**, *101*, 664

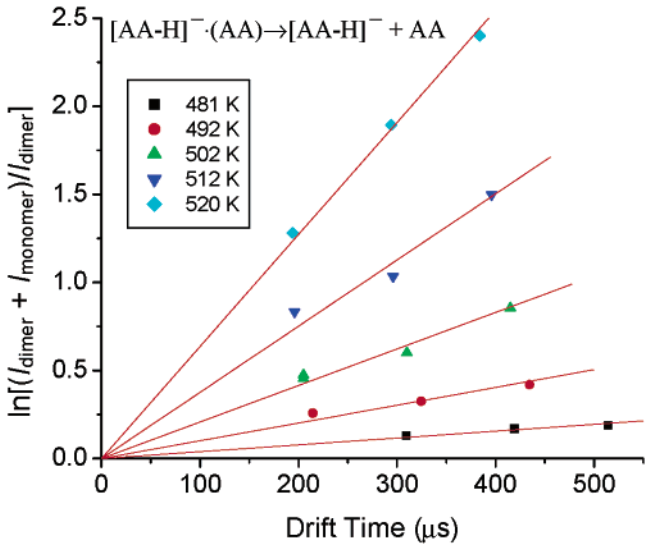

Figure 3. Kinetic data for deprotonated dialanine dimer dissociation at different drift cell temperatures. The slopes of each line are equal to the rate constant at the indicated temperature.

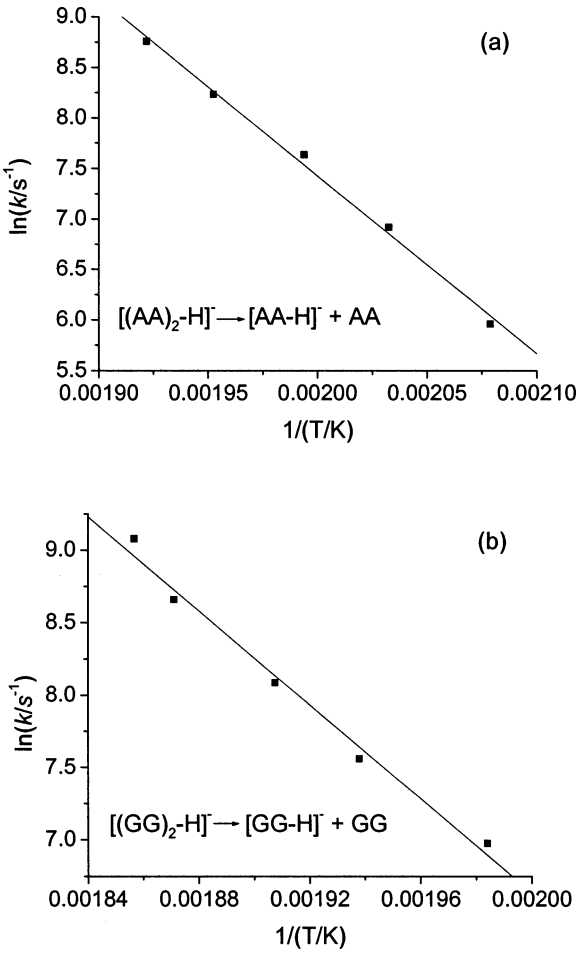

Figure 4. Arrhenius plots for the dissociation of (a) deprotonated dialanine dimer and (b) deprotonated diglycine dimer.

± 0.3 kcal/mol. If we use the ATD-fitting method, we obtain 23.0 ± 2.3 kcal/mol.

The $[AA-H]^-\cdot(AA)$ and $[GG-H]^-\cdot(GG)$ dissociation activation energies of 34.9 ± 1.4 and 32.2 ± 2.1 kcal/mol, respectively, are very similar, which is perhaps not surprising because the structures of alanine and glycine differ only by the

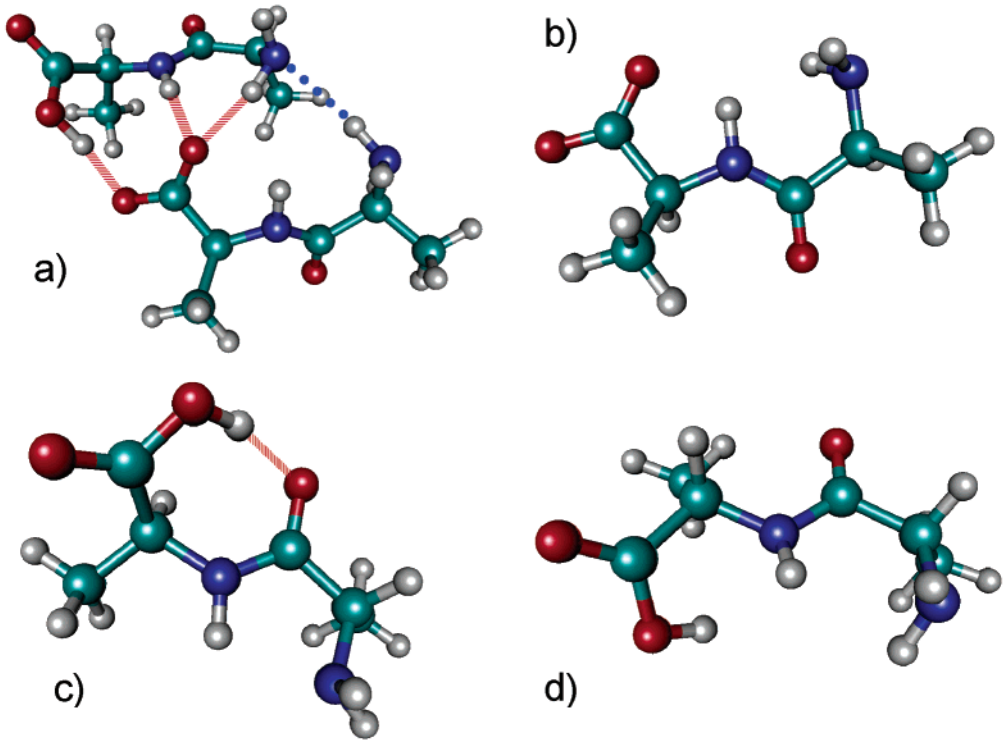

Figure 5. Optimized DFT structures for (a) deprotonated dialanine dimer $[AA-H]^-\cdot(AA)$ (lowest-energy structure), (b) deprotonated dialanine monomer $[AA-H]^-$ (lowest-energy structure), (c) neutral dialanine monomer AA (lowest-energy, H-bonded structure), and (d) neutral dialanine monomer AA (open structure). Typical hydrogen bonds (<3 Å, 180 ± 25°) are indicated as red dashed lines, loose "hydrogen-bond-like" interactions[48] (<3.5 Å, 180 ± 50°) as blue dotted lines. The white balls are H, the green C, the red O, and the blue N. Graphics generated using VMD.[49]

Table 1. Experimental Activation Energies (E_a) and Preexponential Factors (A) for the Dissociation Reaction $[P_2-H]^- \rightarrow [P-H]^- + P$

peptide (P)	E_a (kcal/mol)[a]	log(A/s^{-1})[a]
dialanine (AA)	34.9 ± 1.4	18.5 ± 0.6
diglycine (GG)	32.2 ± 2.1	17.0 ± 0.9

[a] The errors reported here are from the standard deviations of the linear least-squares fits to the experimental data.

substitution of a hydrogen for a methyl group. This similarity in activation energy and A factors suggests that their dissociations have similar reaction paths with similar transition states. Information on the nature of the transition states can be obtained by examining the experimental data in comparison with DFT calculations for the deprotonated dipeptide dimers and monomers.

Directly determining the correct dissociation transition states and their energies using DFT is prohibitively difficult. Instead we approach the problem by calculating the minimum and maximum values for the activation energy for dissociation of the deprotonated dimers. By comparing the experimental activation energy to the calculated minimum and maximum values, we can infer structural information about the real transition states.

The minimum value for the activation energy is the actual dissociation energy for the dimer. This value was calculated for both dialanine and diglycine using a combination of molecular mechanics and DFT to determine energies and structures of species involved in reaction 1. Figure 5a shows the optimized structure for the deprotonated dialanine dimer. This lowest-energy dimer structure has three hydrogen bonds shown as red dashed lines in the figure. This arrangement of hydrogen bonds ensures that the carboxylic group of the deprotonated dialanine subunit, which carries the negative charge for the ion, is very well solvated by the neutral subunit. The cross section calculated for this structure of 116 Å^2 is in good agreement with experiment (118 ± 2 Å^2), giving confidence in the calculations.

The optimized structure for the deprotonated dialanine monomer shown in Figure 5b has a cross section of 69 Å^2 in agreement with the experimental value of 70 ± 3 Å^2. It is very similar to the deprotonated dialanine subunit in the dimer, indicating that few structural changes occur in the deprotonated subunit during dissociation. However the optimized global minimum structure for neutral dialanine monomer (Figure 5c) is quite different from the structure of this moiety in the dimer. The optimized neutral monomer has the N−C_α bond of its second residue rotated to allow the hydroxyl group of the C-terminus to form a hydrogen bond with the carbonyl oxygen of the first residue. We will refer to this neutral structure type as "H-bonded".

According to the DFT calculations, the deprotonated dimer is 24.3 kcal/mol more stable than the separated neutral H-bonded and deprotonated monomers. The dimer is much more stable because the charge site is solvated in the dimer but not at all in the deprotonated monomer. This relative stability is in agreement with our experimental observation that only dimer ions are produced by the ESI source. The calculated value of 24.3 kcal/mol is the minimum energy change for the dissociation reaction (i.e. the bond dissociation energy) and is less than the experimental dissociation activation energy of 34.9 kcal/mol.

DFT calculations were also performed to determine the structures and energies of the deprotonated diglycine dimer, the deprotonated monomer, and neutral monomer. The results are

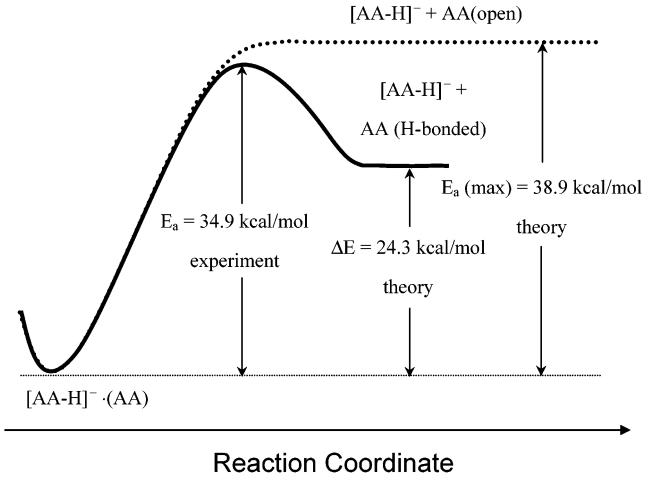

Figure 6. Schematic reaction coordinate diagram for deprotonated dialanine dimer dissociation, $[AA-H]^-\cdot(AA) \rightarrow [AA-H]^- + AA$, illustrating the experimental activation energy and the DFT dissociation energy (solid line). The dashed line represents dissociation to $[AA-H]^-$ and the open form of AA.

similar to those obtained for the dialanine species and therefore are not shown here but are available in Supporting Information.

What is the maximum value possible for the activation energy? As the dissociation proceeds and the distance between two monomer subunits is increased, each monomer subunit will begin to rearrange and stabilize its structure until the transition state is reached. Although we cannot model this process exactly, we can approximate it in our calculation by freezing the structures of both the deprotonated and neutral dialanine subunits of the dimer as they separate. When the two subunits are at infinite distance from one another, all interactions between them are removed. The energy change of 38.9 kcal/mol we calculated for this process is the maximum possible value for the activation energy.[44] The resulting neutral structure (Figure 5d) will be termed "open" to distinguish it from the H-bonded structure.

If the DFT calculations are reasonably accurate, the activation energy should be between the minimum of 24.3 kcal/mol and the maximum of 38.9 kcal/mol. Figure 6 shows the relative energies of this dissociation in a schematic reaction coordinate diagram. The solid line in the diagram illustrates the experimental activation energy of 34.9 kcal/mol and the theoretical dissociation energy of 24.3 kcal/mol. The dashed line shows the theoretically obtained maximum for the activation energy. The theoretical maximum of 38.9 kcal/mol is very similar to the experimental activation energy. This indicates that the true transition state is well-described by the maximum activation energy scenario in which the hydrogen bonds are in the process of being broken with little intramolecular rearrangement of two monomer subunits.

Similar calculations were carried out to determine the maximum possible activation energy for deprotonated diglycine dimer dissociation. The results and the schematic reaction coordinates diagram are similar to the dialanine system and are given in Supporting Information.

Noncovalent Bonds between Peptides and Water Molecules. The second way to stabilize the charge on deprotonated AA and GG is to hydrate them. To investigate this process

(44) The separated "frozen" structures are subjected to DFT minimization to obtain the structures shown in Figure 5b,d.

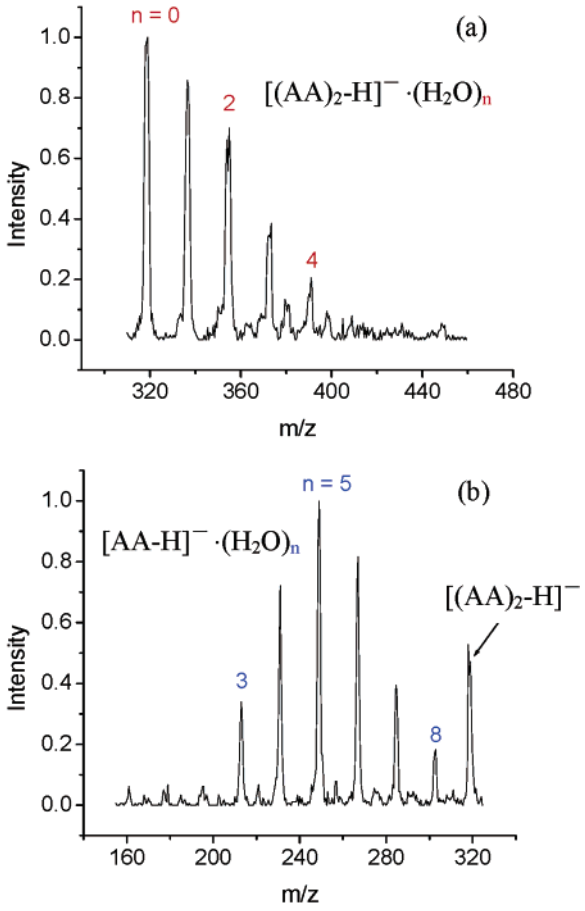

Figure 7. Mass spectra of deprotonated dialanine (a) dimer and (b) monomer after exposure to 1.3 Torr of water vapor at 260 K. The numbers above the peaks indicate the number of water molecules added.

(reaction 2), the deprotonated dimer ions were injected into the drift cell at high energy yielding monomer $[P-H]^-$ ions by collision induced dissociation. Figure 7 shows mass spectra obtained with 1.3 Torr of H_2O in the cell at 260 K under these high-injection-energy conditions. The peaks in each spectrum are labeled with their corresponding n value. Both the dialanine and diglycine dimers can add four or five water molecules under these drift-cell conditions. The monomers, despite their smaller size and the fact that they have fewer hydrophilic groups than the dimers, can add as many as eight or nine water molecules.

Thermodynamic information about the hydration reactions was obtained in temperature-dependent equilibrium experiments. Standard-state free energies, ΔG_n°, were determined, as described in Methods, over a range of temperatures for sequential clustering of water to the peptide ions. Due to experimental constraints (limited P, T range; see Methods), ΔG_n° was only measured for $n = 1-4$ for $[AA-H]^-$ and $[GG-H]^-$, and $n = 1$ for $[AA-H]^-\cdot(AA)$ and $[GG-H]^-\cdot(GG)$. These data are plotted in Figure 8. The ΔH_n° and ΔS_n° values determined from these plots are collected in Table 2. For $[AA-H]^-$, the bond energy for the first water molecule is 11.7 kcal/mol, with each additional H_2O group binding 1−2 kcal/mol more weakly. These values are in reasonable agreement with those calculated by DFT, also shown in Table 2. A similar pattern in the experimental bond energies is observed for $[GG-H]^-$. For the dimers the first water is bound more weakly at 8.4 and 7.5 kcal/mol for dialanine and diglycine, respectively. Good agreement is obtained with theory.

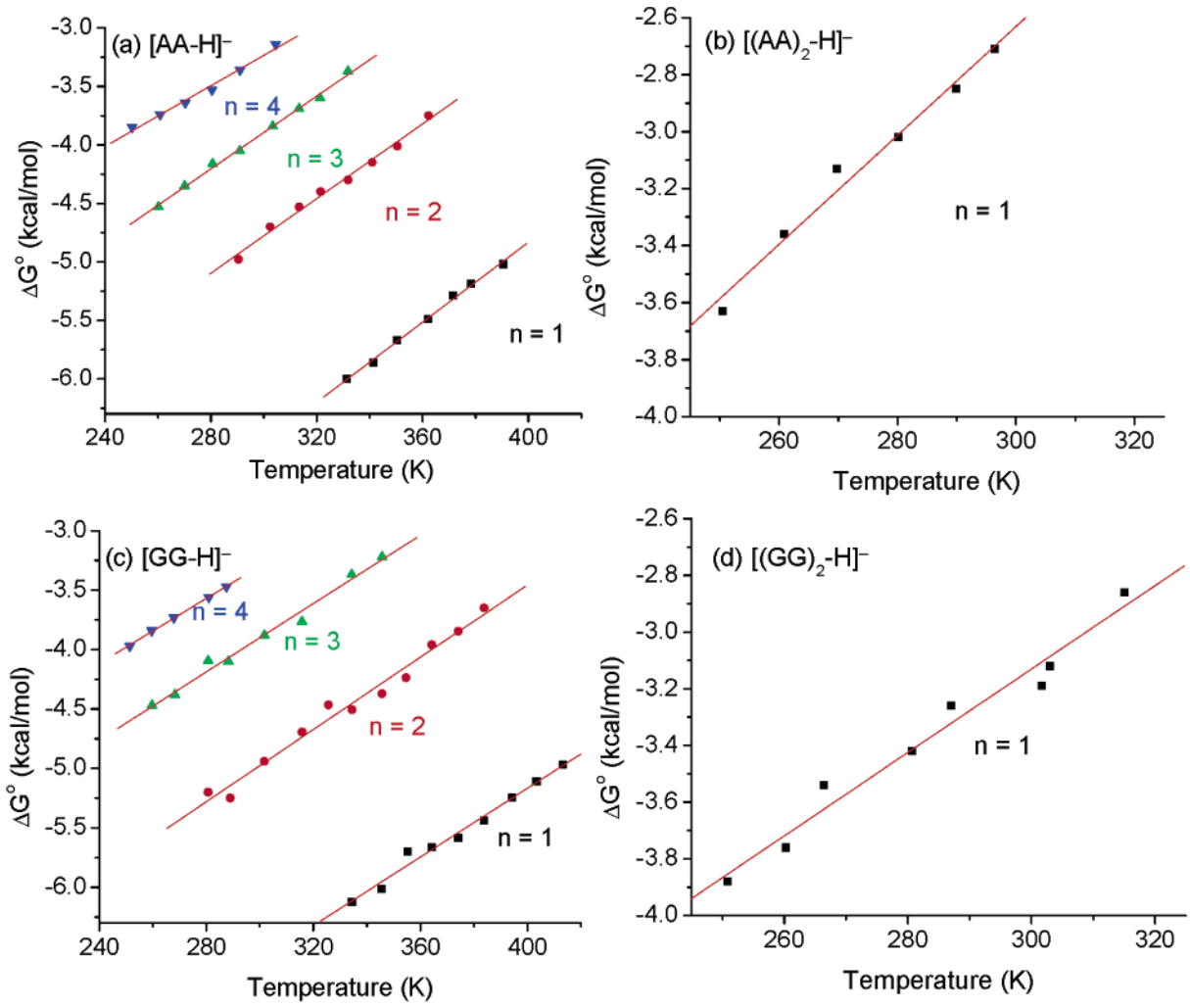

Figure 8. Plots of $\Delta G_n°$ of hydration vs temperature for hydration reactions of the form $[P_{1,2}-H]^-\cdot(H_2O)_{n-1} + H_2O \rightleftharpoons [P_{1,2}-H]^-\cdot(H_2O)_n$ for the deprotonated peptide monomer and dimers (a) $[AA-H]^-$, (b) $[(AA)_2-H]^-$, (c) $[GG-H]^-$, and (d) $[(GG)_2-H]^-$.

Table 2. Theoretical Binding Energies E_n and Experimental $\Delta H_n°$ and $\Delta S_n°$ Values for the Sequential Peptide Hydration $[P_{1,2}-H]^-\cdot(H_2O)_{n-1} + H_2O \rightleftharpoons [P_{1,2}-H]^-\cdot(H_2O)_n$

peptide	n	$-E_n$[a] (kcal/mol)	$-\Delta H_n°$[b] (kcal/mol)	$-\Delta S_n°$[b] [(cal/mol)/K]
$[AA-H]^-$	1	15.6	11.7 ± 0.2	17.1 ± 0.4
	2	12.0	9.6 ± 0.2	16.0 ± 0.6
	3	12.6	8.6 ± 0.2	15.6 ± 0.4
	4		7.1 ± 0.2	13.0 ± 0.7
$[AA-H]^-\cdot(AA)$	1	9.5	8.4 ± 0.4	19.1 ± 1.3
$[GG-H]^-$	1	15.8	11.0 ± 0.3	14.5 ± 0.7
	2	12.1	9.5 ± 0.3	15.2 ± 0.7
	3	12.7	8.2 ± 0.3	14.4 ± 0.7
	4		7.4 ± 0.1	13.7 ± 0.3
$[GG-H]^-\cdot(GG)$	1	8.4	7.5 ± 0.3	14.7 ± 1.1

[a] DFT hydration sites (B3LYP/6-31G*) shown in Figure 9a−c (monomer) and 9f (dimer). [b] The errors reported here are from the standard deviations of the linear least-squares fits to the experimental data.

Entropy changes as a result of hydration are negative (Table 2), because the loss of three translational and three rotational degrees of freedom outweighs the gain in vibrational entropy. Experimental $\Delta S_n°$ values range from −19 to −13 (cal/mol)/K per water molecule added for the systems studied here. For a given system $\Delta S_n°$ values correlate with the corresponding $\Delta H_n°$ values with large binding energies resulting in large entropy changes, a result consistent with earlier results on hydration of protonated peptides.[29]

Figure 9 shows the structures for deprotonated dialanine monomer with up to five water molecules and deprotonated dialanine dimer with one water molecule. A combination of molecular mechanics (MM) and DFT was used to calculate the structures, except for $n = 4$ and 5 where only MM was used. The first water molecule coordinates to both carboxylic oxygens of the C-terminus of the peptide in its lowest energy structure. Normally, hydrogen bonds prefer to be linear, but the symmetry of the deprotonated carboxyl group prevents that from happening in this case. Linear hydrogen bonds can be formed by bridging the H_2O molecule between one carboxyl oxygen and the N-terminal nitrogen. DFT calculations indicate this bridged structure is 2.5 kcal/mol higher in energy than the structure shown in Figure 9a. A structure with water coordinating to only one oxygen of the carboxyl group in a linear arrangement is 3.7 kcal/mol less stable than the structure in Figure 9a and converts without barrier to it.

The structure for $[AA-H]^-\cdot(H_2O)_2$ is shown in Figure 9b. The second water molecule bridges the C- and N-termini in a manner similar to the first water in the positive cluster $[AA+H]^+\cdot(H_2O)$.[29] In $[AA-H]^-\cdot(H_2O)_3$ (Figure 9c), the third water molecule inserts between the first two waters, forming hydrogen bonds with both. The fourth (Figure 9d) and fifth (Figure 9e) waters add to deprotonated dialanine forming a

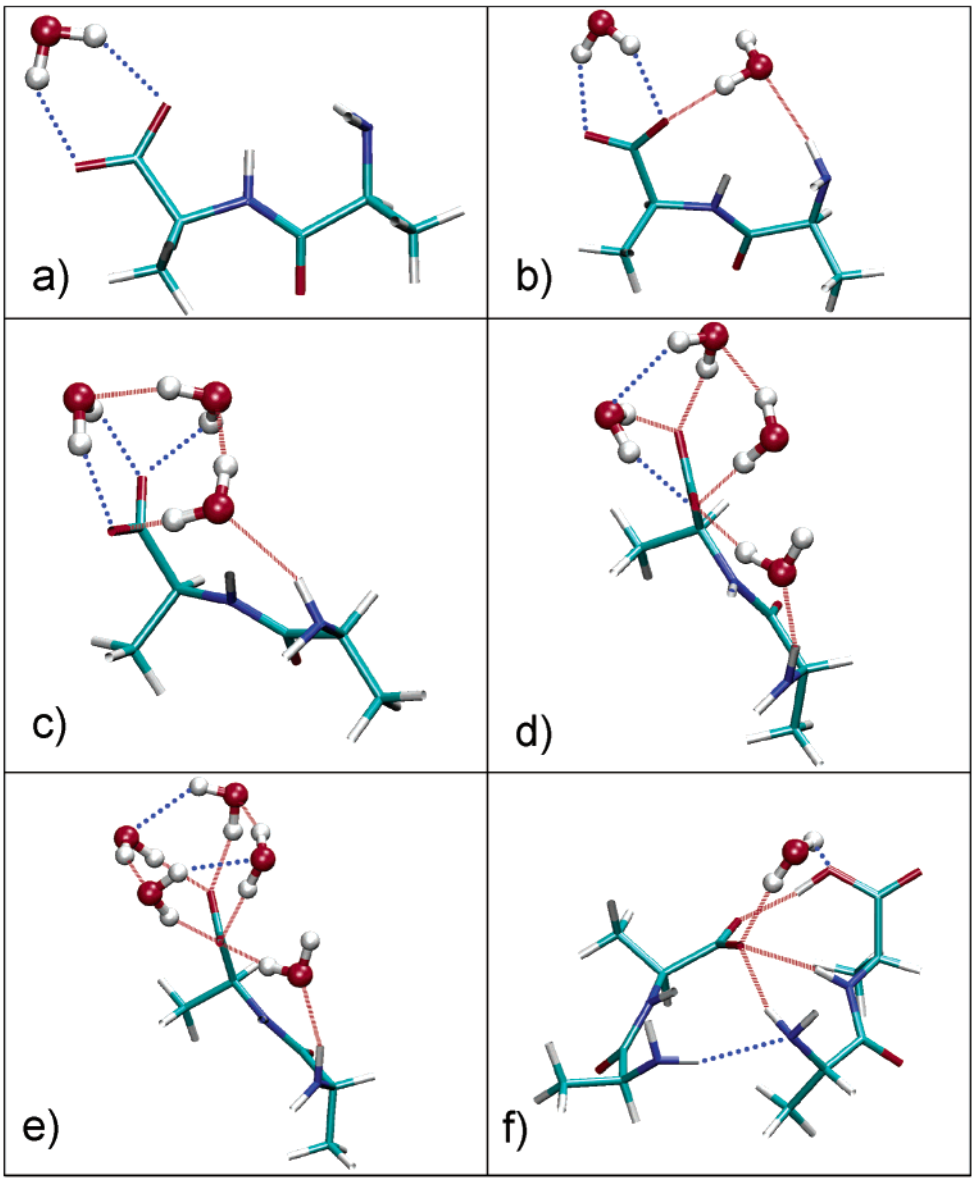

Figure 9. Optimized theoretical structures of $[AA-H]^-\cdot(H_2O)_n$ for (a) $n = 1$, (b) $n = 2$, (c) $n = 3$, (d) $n = 4$, (e) $n = 5$ and (f) for $[(AA)_2-H]^-\cdot(H_2O)$. All calculations included an AMBER simulation followed by a DFT optimization except for $[AA-H]^-\cdot(H_2O)_4$ and $[AA-H]^-\cdot(H_2O)_5$ which are the result of an AMBER simulation only. Typical hydrogen bonds (<3 Å, 180 ± 25°) are indicated as red dashed lines and loose "hydrogen-bond-like" interactions[48] (<3.5 Å, 180 ± 50°) as blue dotted lines. Graphics generated using VMD.[49]

solvation cage around the C-terminus, with one water bridging to the N-terminus. The results shown in Figure 9 indicate that the charge site predominantly controls the solvation process, a phenomenon similar to what has been observed in previous hydration studies of small positively charged protonated peptides.[29]

The structure for deprotonated dialanine dimer hydrated with one water molecule is shown in Figure 9f. As can be seen in Figure 5a, the charge-carrying group in the deprotonated dimer without water is well-solvated by the neutral monomer subunit with three hydrogen bonds, thereby weakening the interaction between the water molecule and the charge-carrying carboxylic group. Hence, while the first water molecule can access the deprotonated carboxyl group, further hydration is made difficult since the neutral dialanine monomer prevents access to the charge-carrying group. This effect is evident in the experimental data. While the monomer can add eight or nine water molecules at 260 K and 1.3 Torr of water, the dimer can add only four water molecules.

Stabilization of the Charge: Self-Solvation vs Hydration vs Dimerization. Very generally, a common structural motif of flexible medium-sized polyatomic ions (~100 atoms) is that the charge carrying unit(s) (carboxylate in this case) is buried in the interior of the molecule, well-self-solvated.[45] However, the dipeptide monomer systems of this study appear to be too small (and/or too rigid) to accomplish efficient self-solvation of the charge (Figure 5b). Hence, the negative charge on the molecule is fully exposed and available for interaction with other molecules. This situation is similar to the totally unshielded charge on sodium (and other metal) ions, which are routinely found to bind to many types of ligands available in the electrospray process.[46]

The large activation energy for dimer dissociation of 35 kcal/

(45) Wyttenbach, T.; Bowers, M. T. *Top. Curr. Chem.* **2003**, *225*, 207.

mol (Figure 6) helps the dimer ions to survive on their journey from the source through the ion funnel and the drift cell to the detector. In contrast, hydrated dimer ions probably lose their solvent molecules one by one on this journey and cannot replenish them due to lack of water in the ion funnel. In addition, neither solvated nor naked monomer ions $[P-H]^-$ are observed at low injection energies, indicating that neither water nor acetonitrile solvation successfully compete with dimerization in the source. Acetonitrile, which lacks acidic hydrogens, is perhaps not surprisingly a poor solvent of the carboxylate group. But water, available in great abundance, should be a competitor with the neutral peptide for solvating the ion.

Because of its larger size the peptide molecule is obviously a better solvent than one water molecule. But why is it better than an unlimited number of water molecules? Energetically it appears as few as four water molecules should be able to compete with one AA (or GG). Yet no deprotonated monomer is observed. The only possible answer is entropy. From Table 2 we can calculate $\Delta G^\circ_{300} = -18.5$ kcal/mol for hydration of $[AA-H]^-$ with four water molecules. A similar calculation[47] yields $\Delta G^\circ_{300} \cong -16$ kcal/mol for solvation of $[AA-H]^-$ by a single AA molecule favoring the hydrated monomer. Of course the dimer will also be hydrated. Judging from the values of ΔH° in the table, one or two water molecules should be added to make a valid comparison with the monomer hydration by four water molecules. Each additional water will add -3 to -4 kcal/mol to ΔG°_{300} for the dimer. Hence adding one water molecule gives $\Delta G^\circ_{300} = -19$ kcal/mol and two water molecules give $\Delta G^\circ_{300} = -22$ kcal/mol. Further hydration to both monomer and dimer should be roughly equivalent. This calculation, though approximate, supports the fact entropy drives the system to essentially pure dimer, consistent with experimental observation.

The calculated potential energy values shown in Figure 6 can be used to compare hydrogen bonding in the dimer with the hydrated monomer. The calculated interaction energy between the neutral AA and the deprotonated AA within the dimer ion is 38.9 kcal/mol. Hence the four hydrogen bonds holding this structure together have an average strength of 9.7 kcal/mol. On the other hand, the four hydrogen bonds[48] in the doubly hydrated monomer system (Figure 9b) have an average strength of 6.9 kcal/mol, substantially weaker than the four hydrogen bonds in the dimer. Hence four or more water molecules are needed to provide the same degree of charge stabilization in the deprotonated monomer as the AA molecule.

(46) *Electrospray Ionization Mass Spectrometry*; Cole, R. B., Ed.; Wiley: New York, 1997.
(47) The entropy change associated with dimerization was assumed to be -30 (cal/mol)/K, nearly double the entropy change for adding a single H_2O molecule to the deprotonated monomer. Entropy change scales with binding energy, and since the dialanine dimer is bound more than twice as strongly as each water of hydration, an entropy change 75% larger is not unreasonable. This magnitude of entropy change is also consistent with the much larger change in rotational entropy occurring on dimerization as compared to hydration, the dominate difference in the two processes.
(48) The term "hydrogen bond" is used here very loosely to describe any pairwise interaction between an electron-pair-accepting hydrogen atom and an electron-pair-donating atom without necessarily fulfilling the usual geometrical requirements (length $\sim$ 2 Å; angle $\sim$ 180°) used to define a hydrogen bond.
(49) Humphrey, W.; Dalke, A.; Schulten, K. *J. Mol. Graphics* **1996**, *14*, 33.

Conclusions

The noncovalent interactions between a peptide and water (hydration) and between two peptide molecules (aggregation) were studied for the small model systems dialanine and diglycine. Our findings are as follows.

1. Electrospraying solutions of the peptides P (dialalanine or diglycine) in the negative ion mode produces exclusively the deprotonated dimers $[P-H]^-\cdot(P)$. Monomer ions $[P-H]^-$ can be generated by high-energy injection of the dimer into the drift cell.

2. MM and DFT calculations indicate that the charge in $[P-H]^-$ is poorly shielded and readily available for noncovalent interaction with other molecules.

3. Hydration mass spectra, along with theoretical results, indicate that the degree of charge solvation achieved by four water molecules, $[P-H]^-\cdot(H_2O)_4$, is similar to that in the dimer, $[P-H]^-\cdot(P)$. Theory indicates that, in both cases, the first solvation shell of the $[P-H]^-$ charge is nearly full.

4. Experimental values for ΔH° of hydration determined for the dialanine system are very similar to those of diglycine. Values range from -11.7 kcal/mol for the first water molecule to -7.1 kcal/mol for the fourth water adding to $[AA-H]^-$. Water molecules adding to the dimer ion are more weakly bound, e.g. 8.4 kcal/mol for the first water bound dialanine dimer due to prior stabilization of the charge in $[AA-H]^-$ by neutral AA.

5. MM and DFT calculations on hydrated $[AA-H]^-$ indicate that the first water molecule binds simultaneously to both oxygen atoms of the carboxylate forming two loose H-bonds, whereas the second water inserts between the C- and N-terminus forming two typical linear hydrogen bonds. The next three water molecules add to the carboxylate oxygens forming a network of eight H-bonds, four to the carboxylate and four from one water to the next in a circular arrangement.

6. MM and DFT calculations on the dimers indicate that the neutral subunit P changes geometry from an H-bonded structure in the unbound state to an open structure within the dimer. The ionic unit $[P-H]^-$ does not significantly change geometry upon aggregation with the neutral unit P.

7. Both $[P-H]^-$ and P subunits in the transition state retain the structures they have in the dimer. Upon complete separation the P subunit relaxes to a new global minimum over 10 kcal/mol lower in energy, but the deprotonated monomer changes structure very little.

8. The absence of monomer $[P-H]^-$ in the solution being sprayed is due to the fact the $[P-H]^-\cdot(P)$ dimer is entropically favored over the hydrated deprotonated monomer.

Acknowledgment. The support of the National Science Foundation under Grant CHE-0140215 is greatly acknowledged.

Supporting Information Available: DFT structures for $[GG-H]^-\cdot(GG)$ and $[GG-H]^-$ and GG and schematic reaction coordinate diagram for $[GG-H]^-\cdot(GG)$ dissociation. This material is available free of charge via the Internet at http://pubs.acs.org.

JA0393628